❏    121

# Quantitative feedback theory based robust speed control of vector controlled induction motor

**Jisha Lakshmi Krishnankutty[1], Arekkadan Antony Powly Thomas[2], Suresh Srivastava[3]**
[1]Department of Electrical and Electronics Engineering, Presidency University, Bangalore, India
[2]Gopalan College of Engineering and Management, Bangalore, India
[3]Defence Research and Development Organisation, Bangalore, India

## ABSTRACT

In this research paper a method for the robust speed control of Indirect Field orient controlled induction motor (IM) is proposed. The quantitative feedback theory (QFT) in implemented to design the controller in order to achieve the desired performance for the closed loop system in the presence of uncertainties and parameter variations. In this research work the QFT based controller is designed for the simplified model of IM. The worst case of uncertainties and all possible parameter variations are taken into consideration. The IM with the controller developed is simulated using the MATLAB/Simulink and the results are analyzed and compared with the conventional proportional integral derivative (PID) controller. The time domain and frequency domain analysis of both controllers were conducted and compared. A study on the nature of electromagnetic torque and control signal is also included to justify the effectiveness of proposed controller. The simulation results verify the superior performance of the proposed robust control method compared to PID controller.

*Corresponding Author:*

Jisha Lakshmi Krishnankutty
Department of Electrical and Electronics Engineering, Presidency University
Bangalore, Karnataka, India
Email: jisha@presidencyuniversity.in

## 1.    INTRODUCTION

Electrical drives play major role in modern industries and automation processes especially where the accurate speed control is the main requirement. With the advancement of power electronic technologies, a digital signal processor (DSP) and micro controllers, and the development of many control algorithm in the speed control field, the performance of AC speed regulation system is becoming more and more superior. With the implementation of vector control scheme [1], the induction motor (IM) decouples the torque and flux, so that the control is possible as simple as DC motor. In the last few years conventional controllers using proportional integral (PI) and proportional integral derivative (PID) control were broadly used for controlling the speed of AC drives due to its simplicity and better performance. But the behavior of these system with conventional controllers may not preserve the robustness in the presence of parameter variations and external disturbances. Therefore, the concept of robust control gained more interest in the field of control of AC drives. The IM is highly coupled, nonlinear and multivariable system and the variation is machine parameters with saturation, temperature and skin effect add further nonlinearity to the machine model. The quantitative feedback theory (QFT) is a unified theory which emphasize using feedback to meet the desired performance specifications even in the presence of uncertainties and disturbances.

Horowitz [2] introduced the concept of QFT, which clearly highlights how feedback can be used to overcome the effect of plant uncertainties and meet the performance specifications. The design of QFT based

controller involves typical frequency response analysis involving Bode diagrams, generating templates and Nichols charts (NC). The QFT is based on the fact that the feedback is needed principally when the model uncertainty or the uncertain disturbances acting on the plant exceed the permissible limit. A study on the evolution of QFT is described in the papers written by Horowitz [3], Houpis [4], and Garcia-San [5]. The major analysis of QFT can be found in the books written by Houpis *et al.* [6], Yaniv [7], and Sidi [8]. In Yaniv and Boneh [9] proposed a robust method of lifetime value (LTV) feedback synthesis for SISO nonlinear plants [9].

In the literature, there are several real time applications of QFT listed [10]–[13]. Garcia-Sanz *et al.* [14] proposed "design of QFT non-diagonal controllers for use in uncertain multiple-input multiple-output systems". Qi *et al.* [15] proposed "robust control based on QFT for permanent magnet synchronous generator (PMSG) wind power generation system". Garcia-Sanz *et al.* [16] developed high-performance switching QFT control for large radio telescopes with saturation constraints. Yazan *et al.* [17] proposed the "development of robust QFT controller for quanser bench-top helicopter". Sharma and Pratap [18] developed robust controller for twin rotor system using QFT and in [19] a robust engine speed controller is designed based on QFT, by Lu *et al.* [20] QFT can also be applied for course control of marine oil tanker, automated control of photovoltaic converter [21], and control synthesis of tracking error problem [22].

The objective of the research work is to design the prefilter *F(s)* and the controller *G(s)* as shown in Figure 1 so that the specified robust design is achieved for the given region of plant parameter uncertainty. *P(s)* represents the plant transfer function, *R(s)* is the reference input, *Y(s)* is the output and *D* represents the external disturbance. The control objectives defined are, the rise time of the closed loop response $t_r \leq 0.5$ sec, settling time $t_s \leq 2$ sec, gain margin $\geq 10$ dB and phase margin $\geq 20°$.

The section 2 of this article describes the mathematical model of vector controlled IM. The design procedure of the QFT controller is presented in section 3. The simulation results and the discussions are included in section 4.
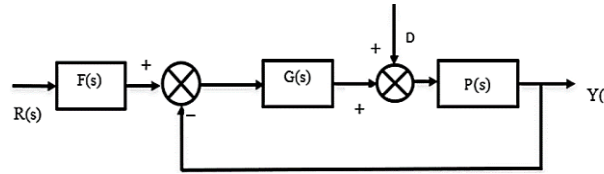


Figure 1. Block diagram of feedback system designed using QFT

## 2. MATHEMATICAL MODEL OF VECTOR CONTROLLED INDUCTION MOTOR

The dynamic model of the IM is based on conversion of a-b-c axes into direct and quadrature axes. By considering all the instantaneous effects due to variation of supply voltage or current, stator frequency and load variations the dynamic model is developed. The dynamic model for the vector-controlled IM in d-q reference frame is given as (1)-(5) [23], [24]. The state variables identified are $i_{ds}$, $i_{qs}$, $\psi_{dr}$, and $\psi_{qr}$.

$$\frac{di_{ds}}{dt} = -\left(\frac{R_s}{\sigma L_s} + \frac{1-\sigma}{\sigma \tau_r}\right) i_{ds} + \omega_e i_{qs} + \frac{L_m}{\sigma L_s L_r \tau_r} \psi_{dr} + \frac{L_m \omega_r}{\sigma L_s L_r} + \frac{1}{\sigma L_s} V_{ds} \tag{1}$$

$$\frac{di_{qs}}{dt} = -\left(\frac{R_s}{\sigma L_s} + \frac{1-\sigma}{\sigma \tau_r}\right) i_{qs} - \omega_e i_{ds} + \frac{L_m}{\sigma L_s L_r \tau_r} \psi_{qr} + \frac{L_m \omega_r}{\sigma L_s L_r} + \frac{1}{\sigma L_s} V_{qs} \tag{2}$$

$$\frac{d\psi_{dr}}{dt} = \frac{L_m}{\tau_r} i_{ds} - \frac{1}{\tau_r} \psi_{dr} + (\omega_e - \omega_r)\psi_{qr} \tag{3}$$

$$\frac{d\psi_{qr}}{dt} = \frac{L_m}{\tau_r} i_{qs} - \frac{1}{\tau_r} \psi_{qr} - (\omega_e - \omega_r)\psi_{dr} \tag{4}$$

$$T_e = \frac{3P}{4} \frac{L_m}{L_r} \left(\psi_{dr} i_{qs} - \psi_{qr} i_{ds}\right) \tag{5}$$

In (1)-(5) $i_{ds}$ and $i_{qs}$ are components of stator current in direct axis and quadrature axis, $V_{ds}$, $V_{qs}$ are d-q components of stator voltage, $\psi_{dr}$, $\psi_{qr}$ are the rotor fluxes in d and q axis. $\sigma = 1 - \frac{L_m^2}{L_s L_r}$ is the leakage coefficient of flux. $L_s, L_r$ & $L_m$ are stator, rotor and mutual inductances. $R_s$ and $R_r$ are stator and rotor resistances. $\omega_e$ and $\omega_r$ are the synchronous speed and the rotor speed respectively in rad/sec. $\tau_r = \frac{L_r}{R_r}$ is the

rotor time constant, $T_e$ , the electromagnetic torque developed in the IM and *P*, number of poles [25], [26]. In the field-oriented control (FOC), to decouple flux and torque, $i_{qs}$ should align in the direction of total rotor flux $\psi_r$ with $i_{ds}$ perpendicular to it. To satisfy this condition, $\psi_{qr}=0$, then, $\psi_{dr}=\psi_r$. Substituting in (6):

$$T_e = K_T i_{qs} \tag{6}$$

where, $K_T = \frac{3P}{4}\frac{L_m}{L_r}\psi_{dr}^*$ and $\psi_{dr}^*$ is the command rotor flux. Slip speed (7),

$$\omega_{sl} = \omega_e - \omega_r = \frac{L_m}{\tau_r}\frac{i_{qs}}{\psi_{dr}} \tag{7}$$

in indirect FOC (8) and (9),

$$\omega e = \omega r + \omega sl \tag{8}$$

$$\theta e = \int \omega e\, dt = \int(\omega r + \omega sl)dt = \theta r + \theta sl \tag{9}$$

## 3. DESIGN OF QFT BASED CONTROLLER

The design of QFT controller is simple and transparent which accepts various tradeoffs from the designer to achieve the closed loop system performance specifications. The QFT design is performed using the Nichols chart (NC). The coordinates of the NC are ($\varphi$, 20log(r)). The horizontal coordinate, $\varphi$, typically ranges between -360 to 0, while the vertical coordinate, 20log(r), ranges theoretically from -∞ dB to +∞ dB. A The computational steps involved in the QFT design are: i) defining model of the plant by considering parameter variations; ii) generation of templates; iii) defining desired performance specifications; iv) generation of robust tracking bounds; v) controller design using loop shaping concept; vi) prefilter design in order to achieve tracking specifications; and vii) performing simulation studies to validate the designed controller.

### 3.1. Plant definition

As step 1, The plant model is defined, and the parameter variations are taken into account. $T_L$ is assumed as zero. The plant transfer function P (s)=$K_T$/((Ra+sLa)(Js+B)) ,where Ra=10.733 Ω, La=0.038 H, J=0.0088 kg/m$^2$ and B=0.003. 5% variation in the Ra, La, J and B parameters are considered for the design of controller. The upper and lower limits of the parameters considered are Ra [9.66, 11.8], La [0.036, 0.0.04], J [0.00836, 0.00924] and B [0.00285, 0.00315]. The frequencies chosen are [0.1, 1, 5, 10, 100, 500, 1,000] rad/sec.

### 3.2. Plant templates

After defining the plant, the next step in the design of QFT is generation of plant templates. As shown in Figure 2, the plant templates are drawn between open loop phase and open loop magnitude of the system for the frequencies starting from 0.1 to 1,000 rad/sec. These templates give the boundary of response for the various operating frequency range [27], [28].
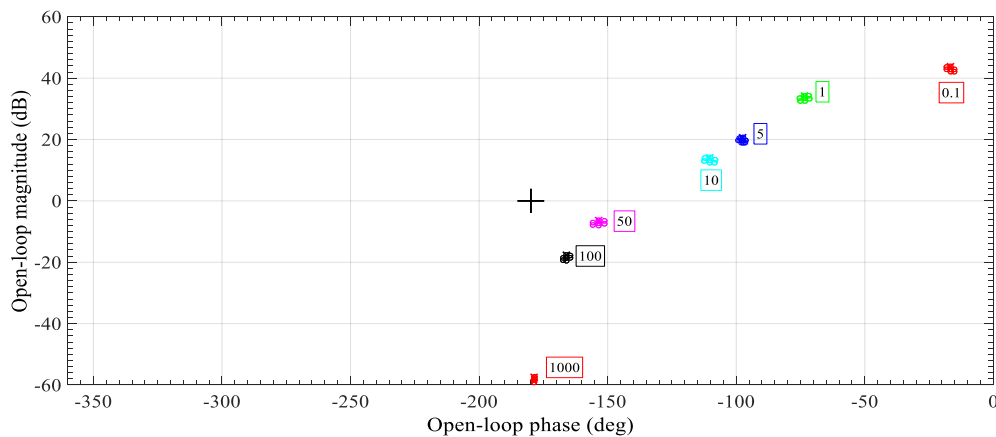


Figure 2. Plant templates for different frequencies

### 3.3. Defining specifications

The next step in the design of QFT controller is to define the specifications based on the performance requirements. In the present design the specifications defined are stability, input disturbance rejection and reference tracking. For the stability specification closed loop constant magnitude of M circle in NC is selected as, *Ws*=1.2, in order to achieve the desired control objectives. Then the corresponding gain margin (GM) and phase margin (PM) are obtained using the 10) and (11) as:

$$Gain\ margin\ =\ 20log\ (1\ +\ \frac{1}{Ws})\ in\ dB \tag{10}$$

$$Phase\ margin\ =\ 180 - 2cos - 1\left(\frac{0.5}{Ws}\right)\ in\ degree \tag{11}$$

based on the performance requirements, upper and lower tracking bounds are fixed based on (12) and (13) as:

$$TRU(s)\ =\ \frac{18s+1200}{s^2\ +40s+1200} \tag{12}$$

$$TRL(s)\ =\ \frac{12000}{s^3+45s^2+1200s+12000} \tag{13}$$

### 3.4. Generating bounds

Next step in the design of QFT is the generation of bounds, corresponding to the defined specifications. The specifications defined in the time and frequency domain decides a minimum damping ratio δ for the dominant roots of the closed loop system and it corresponds to a boundary on M circle which is called stability bounds. This boudary must not be penetrated by the templates and the loop transfer function L(s) for all ω. Bounds are generated for all the frequencies selected and the intersection of all bounds are generated as shown in Figure 3.
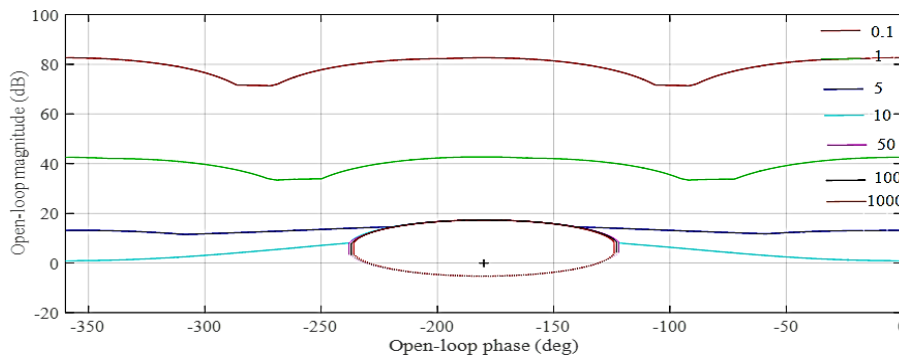


Figure 3. Intersection of all the bounds generated

### 3.5. Design of controller (loop shaping)

The nominal loop, which is the product of the nominal plant transfer function and the controller G(s) which is to be designed, must satisfy the worst case of all the bounds. The design of G(s) requires changing the gain, add poles and zeros either real or complex, until the nominal loop Lo(s) lies above the solid line bounds and below the dashed line bounds at each frequency. The loop Lo(s) in frequency domain along with the bounds superimposed on NC is shown in Figure 4. The controller G(s) is obtained (14) as.

$$G(s)\ =\ \frac{6.72(s+12)(s+15.36)}{s(s+123.9)} \tag{14}$$

### 3.6. Design of prefilter

Once the controller G(s) is designed, next task in 2 degree of freedom (DOF) control structure is to design the prefilter. The purpose of the prefilter is to place the system response within the lower and upper tracking specification. The procedure for the design of prefilter F(s) is same as that of controller G(s). The gain is varied, poles and zeros either real or complex are added so that the system time or frequency response lies

within the upper and lower tracking specifications as shown in Figure 5. Thus, the parameters of the filter transfer function is obtained and is expressed as shown in (15).

$$F(s) = \frac{33.657(s+12)}{(s+44.88)(s+9)}$$ (15)
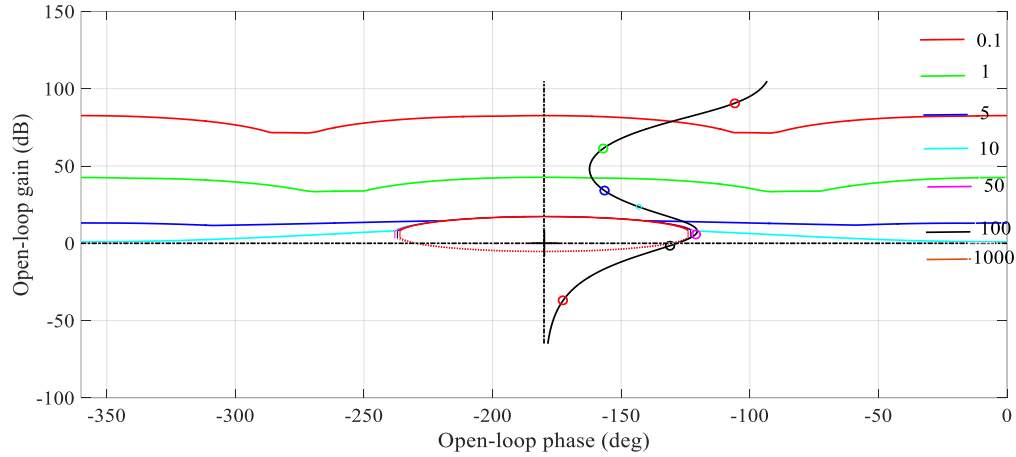


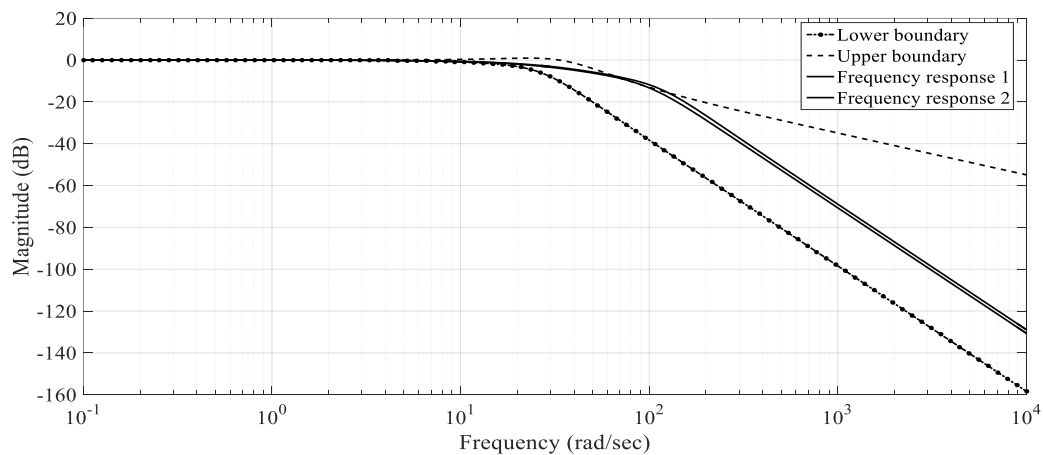Figure 4. Controller design using loop shaping



Figure 5. Prefilter design

### 3.7. Design validation

The analysis of closed loop stability in frequency domain is shown in Figure 6. The dashed line shows the stability specification and solid line shows the worst case of the function $(P_o G)/(1+P_o G)$ at each frequency due to the model uncertainty where $P_o$ represents the plant transferfunction. As the solid line is below the dashed line, the control system meets the stability specifications. The frequency response of the input disturbance rejection of the plant is shown in Figure 7. The dashed line represents the input disturbance boundary. The solid line represents the worst-case input disturbance. The time domain simulations of the closed loop system are shown in Figures 8 and 9. The unit step response of the system which lies between the upper and lower boundaries is shown in Figure 8. The step response is under damped in nature with settling time of 0.18 sec and zero steady state error. The impulse response of the closed loop system is shown in Figure 9. The impulse response settles to zero at 0.2 second, which also indicates closed loop stability.
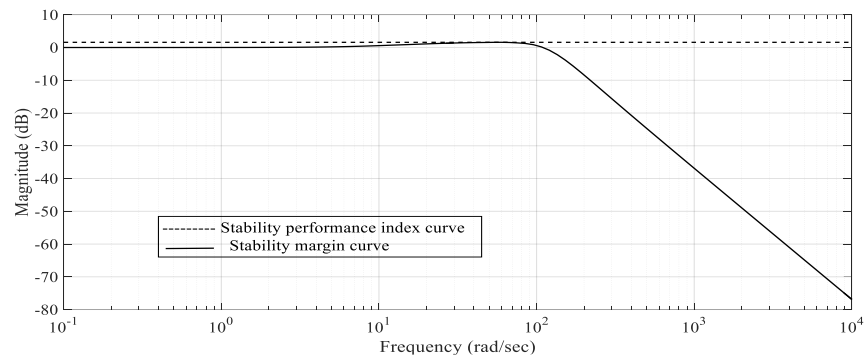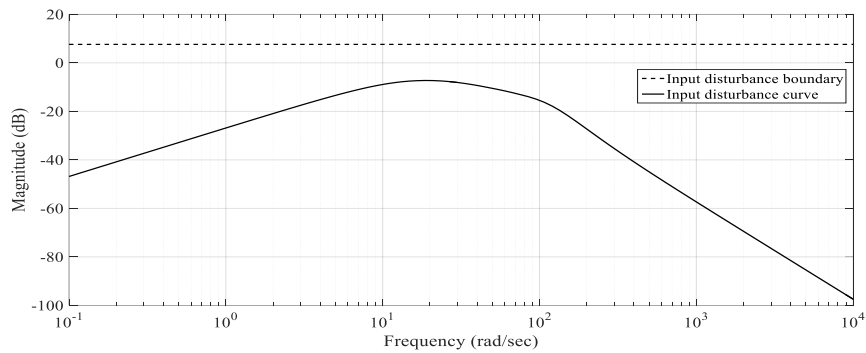
Figure 6. Stability margin
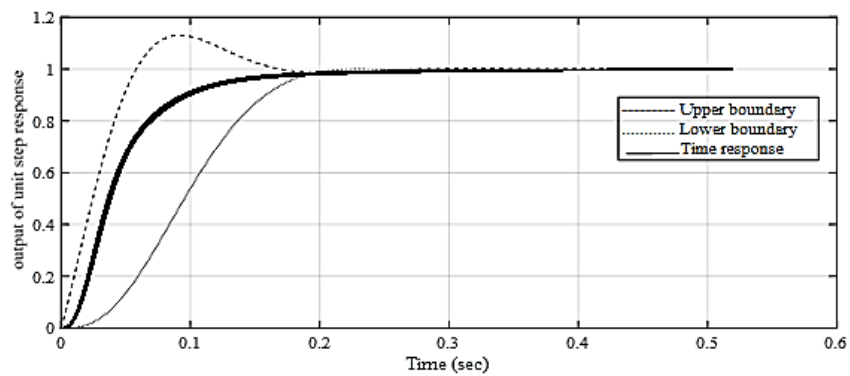


Figure 7. Input disturbance margin



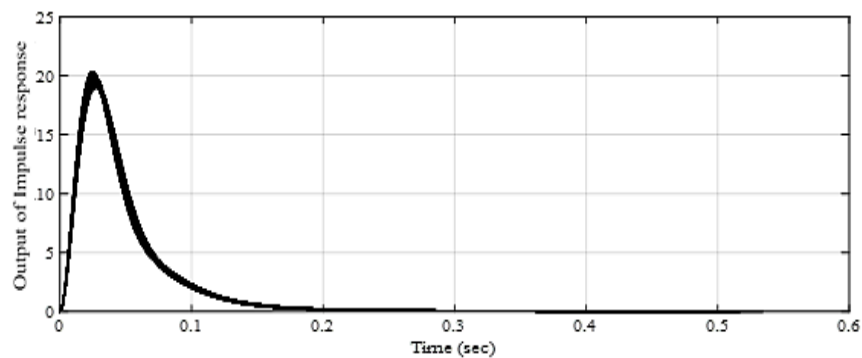Figure 8. Reference tracking boundaries



Figure 9. Impulse response

## 4.     RESULTS AND DISCUSSION

The QFT controller designed is tested with indirect flux-oriented control (IFOC) IM model explained in section 3. MATLAB/Simulink software is used for the simulation studies. The reference speed of 120 rad/sec is selected for the simulation. Simulation studies are carried out under no load condition, a with load, varying the reference speed, and varying the motor parameters. For PID controller the proportional gain constant $K_p$ is fixed to 0.1, Integral gain constant $K_i$ is 0.6 and derivative gain cons tant $K_d$ is 0.001. These constants are initially fixed using Ziegler-Nichols method and is fine tuned using trial and error method to obtain the desired response.

Figure 10 shows the speed–time characteristics of QFT based controller and PID controller without load. The nature of both responses is overdamped. QFT based shows the settling time of 0.15 sec and for PID controller it is 0.2 secs. In both responses steady state error is zero. Figure 11 shows the speed-time response of IM with QFT controller and PID controller when tested with a sudden load of 6 Nm applied at 0.5 sec. It is observed that with QFT controller there is only a negligible drop in speed, around 1 rad/sed at 0.5 sec, the motor picks up its reference speed with zero steady state error. But with PID controller there is a sudden drop is speed to 100 rad/sec. Then due to controller action motor slowly picks up its reference speed. Figure 12 shows the frequency response of PID and QFT controllers. Table 1 compares the time and frequency domain behaviors of both controllers. It shows that QFT is fast acting controller compared to PID controllers. The steady state error with all the controllers is zero. The positive values of GM and PM indicates that, both the controllers ensure stable performance. Figure 13 shows the variation of electromagnetic torque with time at no-load for QFT based controller. The torque initially increases with speed up to 18 Nm then decreases and settles to zero as the speed attains to its steady state value. After settling there is a fluctuation of ±1 Nm. The corresponding variations in control signal is shown is Figure 14. The control effort is required initially as the speed increases. When the motor picks up the speed, the control signal $I_{qs}$ decreases drastically and settles to 1 A. Under noload condition this minor control effort is required to meet the losses of IM. Figure 15 shows the speed–time response when tested with step change in command signal at 0.5 sec. The step change in command speed is introduced at 0.5 sec from 100 to 120 rad/sec. The motor picks up the new speed and settles at 0.6 sec itself.
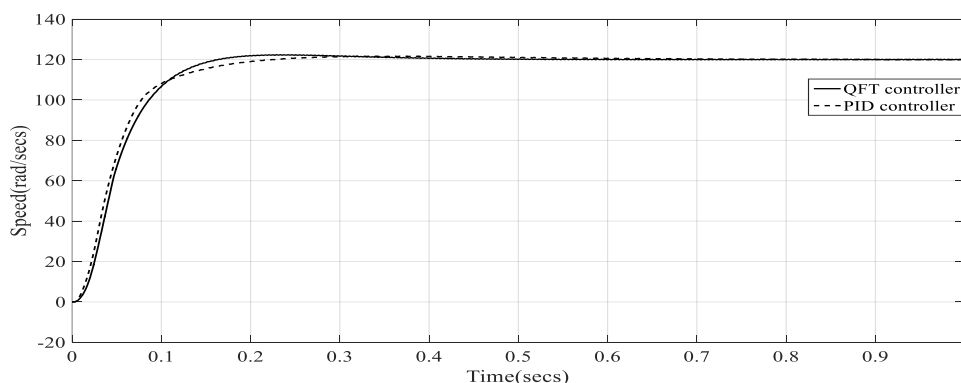


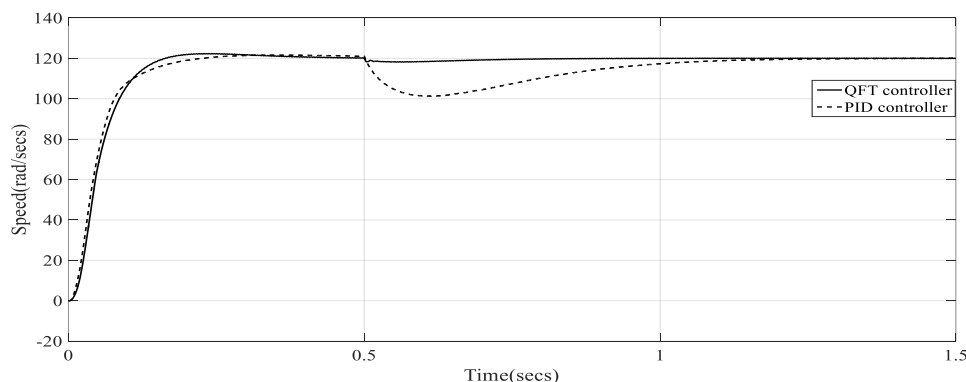Figure 10. Speed-time response of QFT and PID controllers when $T_L$=0



Figure 11. Speed-time response of QFT and PID controllers when $T_L$=6 Nm
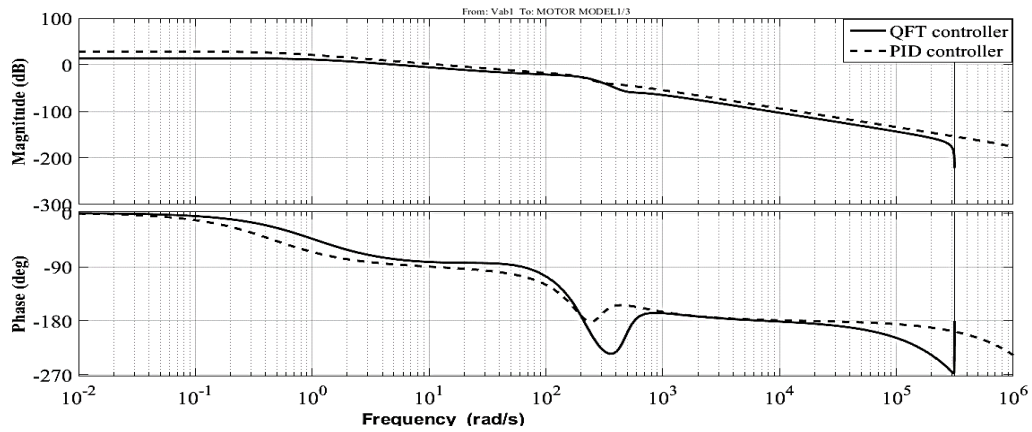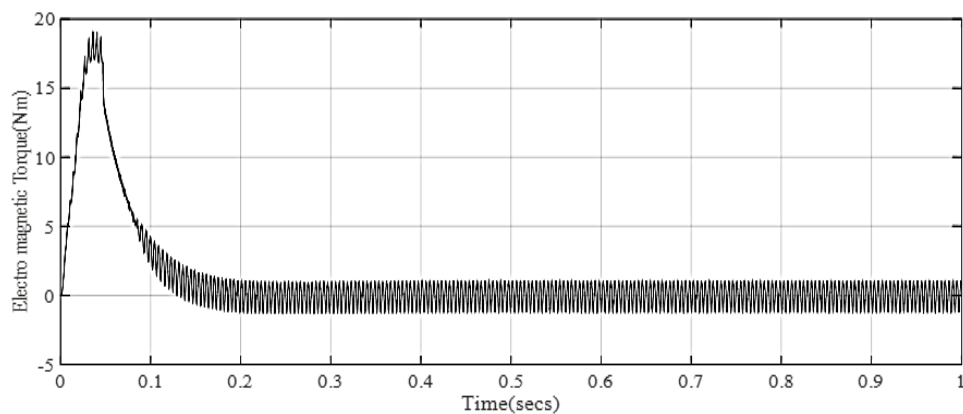
Figure 12. Bode plot of PID and QFT controllers

Table 1. Performance comparison between QFT controller and PID controller

| Controller description | Rise time (secs) | Settling time (secs) | Steady state error (rad/sec) | Gain margin (dB) | Phase margin (degree) |
|---|---|---|---|---|---|
| QFT controller | 0.15 | 0.15 | 0 | 27.4 dB at 211 rad/sec | 102° at 5.26 rad/sec |
| PID controller | 0.2 | 0.2 | 0 | 30.1 dB at 226 rad/sec | 89.2° at 12.6 rad/sec |



Figure 13. Electromagnetic torque-time response with QFT based controller when TL=0
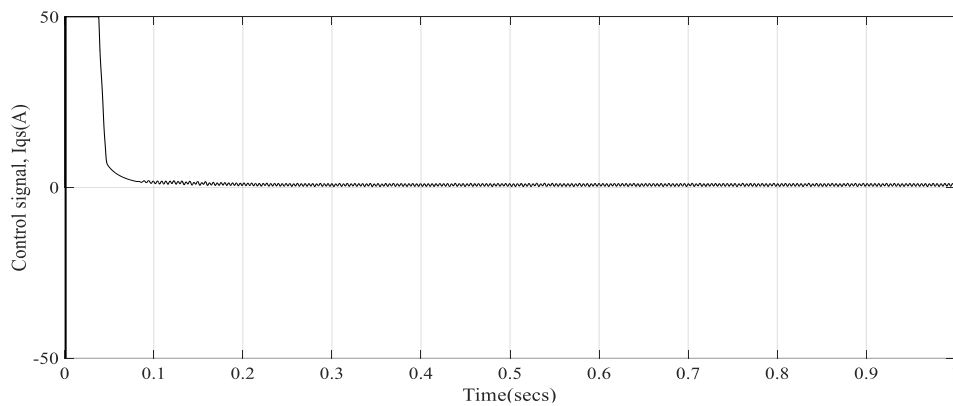


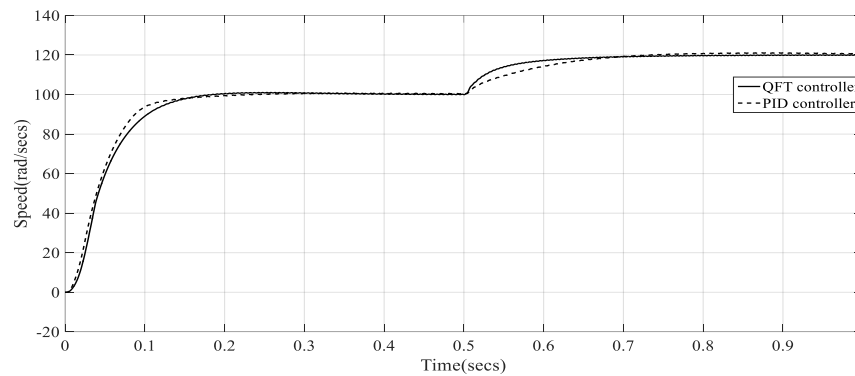Figure 14. Control signal, Iqs-time response with QFT based controller when TL=0

Figure 15. Speed-time response when a sudden rise in command signal at 0.5 sec from 100 to 120 rpm

## 5. CONCLUSION

It is necessary to develop robust controllers for the control of industrial drives as the conventional PID controllers can not assure system performance in the presence of uncertainties. This research paper describes the application of QFT for the robust speed control of IFOC IM. Mathematical model of IFOC IM and the steps involved in the design of QFT controller are explained. The controller and the prefilter designed is tested with full order model of IFOC IM. The performance of both controllers is studied by suddenly varying the load and the reference speed. The time domain analysis and frequency domain analysis of the system validates the robustness of QFT controller compared to conventional PID controller. The smooth variation of torque and control signal shows the superior behavior of QFT controller.

## REFERENCES

[1] F. Blaschke, "The principle of field orientation as applied to the new transvector closed-loop system for rotating-field machines," *Journal of Chemical Information and Modeling*, vol. 34, no. 9, pp. 217–220, 1972.

[2] I. Horowitz, "Fundamental theory of automatic linear feedback control systems," *IRE Transactions on Automatic Control*, vol. 4, no. 3, pp. 5–19, Dec. 1959, doi: 10.1109/TAC.1959.1104893.

[3] I. Horowitz, "Invited paper Survey of quantitative feedback theory (QFT)," *International Journal of Control*, vol. 53, no. 2, pp. 255–291, Feb. 1991, doi: 10.1080/00207179108953619.

[4] C. H. Houpis, R. R. Sating, S. Rasmussen, and S. Sheldon, "Quantitative feedback theory technique and applications," *International Journal of Control*, vol. 59, no. 1, pp. 39–70, Jan. 1994, doi: 10.1080/00207179408923069.

[5] M. Garcia-Sanz, "QFT international symposia: Past, present and future," in *Editorial del 5th Int. Symp. on QFT and Robust Frequency Domain Methods, Pamplona, Spain*, 2001.

[6] C. H. Houpis, S. J. Rasmussen, and M. Garcia-Sanz, *Quantitative feedback theory: Fundamentals and applications*. Boca Raton: CRC Press, 2005.

[7] O. Yaniv, *Quantitative feedback design of linear and nonlinear control systems*. Boston, MA: Springer US, 1999. doi: 10.1007/978-1-4757-6331-7.

[8] M. J. Sidi, *Design of robust control systems: From classical to modern practical approaches*. Malabar: Krieger Publishing Company, 2001.

[9] O. Yaniv and R. Boneh, "Robust LTV feedback synthesis for SISO non-linear plants," *International Journal of Robust and Nonlinear Control*, vol. 7, no. 1, pp. 11–28, 1997, doi: 10.1002/(SICI)1099-1239(199701)7:1<11::AID-RNC199>3.0.CO;2-6.

[10] M. Garcia-Sanz and J. X. Ostolaza, "QFT-control of a biological reactor for simultaneous ammonia and nitrates removal," *Systems Analysis Modelling Simulation*, vol. 38, no. 2, pp. 353–370, 2000.

[11] M. Kelemen and O. Akhrif, "Linear QFT control of a highly nonlinear multi-machine power system," *International Journal of Robust and Nonlinear Control*, vol. 11, no. 10, pp. 961–976, Aug. 2001, doi: 10.1002/rnc.634.

[12] A. E. Bentley, "Pointing control design for a high precision flight telescope using quantitative feedback theory," *International Journal of Robust and Nonlinear Control*, vol. 11, no. 10, pp. 923–960, Aug. 2001, doi: 10.1002/rnc.635.

[13] P. O. Gutman, E. Horesh, R. Guetta, and M. Borshchevsky, "Control of the aero-electric power station – an exciting QFT application for the 21st century," *International Journal of Robust and Nonlinear Control*, vol. 13, no. 7, pp. 619–636, Jun. 2003, doi: 10.1002/rnc.828.

[14] M. Barreras, M. Garcia-Sanz, and I. Egaña, "Design of quantitative feedback theory non-diagonal controllers for use in uncertain multiple-input multiple-output systems," *IEE Proceedings - Control Theory and Applications*, vol. 152, no. 2, pp. 177–187, Mar. 2005, doi: 10.1049/ip-cta:20041186.

[15] C. Qi, M. Tao, and Z. Ji, "Robust control based on quantitative feedback theory for PMSG wind power generation system," in *2009 Chinese Control and Decision Conference*, Jun. 2009, pp. 2122–2127. doi: 10.1109/CCDC.2009.5192312.

[16] M. Garcia-Sanz, T. Ranka, and B. C. Joshi, "High-performance switching QFT control for large radio telescopes with saturation constraints," in *2012 IEEE National Aerospace and Electronics Conference (NAECON)*, Jul. 2012, pp. 84–91. doi: 10.1109/NAECON.2012.6531034.

[17] S. A. S. Yazan, H. Mansor, T. S. Gunawan, and S. Khan, "Development of robust quantitative feedback theory controller for quanser bench-top helicopter," in *2014 IEEE International Conference on Smart Instrumentation, Measurement and Applications (ICSIMA)*, Nov. 2014, pp. 1–4. doi: 10.1109/ICSIMA.2014.7047437.

[18] J. Sharma and B. Pratap, "Robust controller design for twin rotor system using quantitative feedback theory with parametric uncertainty," in *2015 2nd International Conference on Recent Advances in Engineering & Computational Sciences (RAECS)*, Dec.

2015, pp. 1–6. doi: 10.1109/RAECS.2015.7453300.

[19]  L. Lu, Y. Hu, J. Hong, X. Gong, and H. Chen, "Robust engine speed controller design based on quantitative feedback theory," in *2016 12th World Congress on Intelligent Control and Automation (WCICA)*, Jun. 2016, pp. 2365–2369. doi: 10.1109/WCICA.2016.7578740.

[20]  P. Arvind, S. Banerjee, S. Kumari, B. Satpati, and S. Das, "Robust controller design for course changing/ course keeping control of a mariner oil tanker using quantitative feedback theory," in *2017 International Conference on Circuit ,Power and Computing Technologies (ICCPCT)*, Apr. 2017, pp. 1–5. doi: 10.1109/ICCPCT.2017.8074255.

[21]  P. Sutyasadi and M. B. Wicaksono, "Robotic arm joint position control using iterative learning and mixed sensitivity H∞ robust controller," *Bulletin of Electrical Engineering and Informatics*, vol. 10, no. 4, pp. 1864–1873, Aug. 2021, doi: 10.11591/eei.v10i4.3059.

[22]  H. Gudimindla and K. M. Sharma, "Performance analysis of automated quantitative feedback theory based robust controller for photovoltaic converter," in *2018 International Conference on Emerging Trends and Innovations In Engineering And Technological Research (ICETIETR)*, Jul. 2018, pp. 1–7. doi: 10.1109/ICETIETR.2018.8529114.

[23]  R. Jeyasenthil and T. Kobaku, "Quantitative synthesis to tracking error problem based on nominal sensitivity formulation," *IEEE Transactions on Circuits and Systems II: Express Briefs*, vol. 68, no. 7, pp. 2483–2487, Jul. 2021, doi: 10.1109/TCSII.2021.3050994.

[24]  L. K. Jisha and A. A. P. Thomas, "A comparative study on scalar and vector control of Induction motor drives," in *2013 International conference on Circuits, Controls and Communications (CCUBE)*, Dec. 2013, pp. 1–5. doi: 10.1109/CCUBE.2013.6718554.

[25]  A. E. Said and A. M. E. Awwad, "A comparative study of performance of AC and DC electric drive control systems with variable moment of inertia," *Bulletin of Electrical Engineering and Informatics*, vol. 10, no. 2, pp. 588–597, Apr. 2021, doi: 10.11591/eei.v10i2.2768.

[26]  K. S. Reddy and S. B. Veeranna, "Single phase multifunctional integrated converter for electric vehicles," *Indonesian Journal of Electrical Engineering and Computer Science*, vol. 24, no. 3, pp. 1342–1353, Dec. 2021, doi: 10.11591/ijeecs.v24.i3.pp1342-1353.

[27]  K. S. Gaeid, A. F. Nashee, I. A. Ahmed, and M. H. Dekheel, "Robot control and kinematic analysis with 6DoF manipulator using direct kinematic method," *Bulletin of Electrical Engineering and Informatics*, vol. 10, no. 1, pp. 70–78, Feb. 2021, doi: 10.11591/eei.v10i1.2482.

[28]  K. S. Reddy and S. B. Veeranna, "Modified full bridge dual inductive coupling resonant converter for electric vehicle battery charging applications," *International Journal of Power Electronics and Drive Systems (IJPEDS)*, vol. 13, no. 2, pp. 773–782, Jun. 2022, doi: 10.11591/ijpeds.v13.i2.pp773-782.

## BIOGRAPHIES OF AUTHORS

**Jisha Lakshmi Krishnankutty** received her Ph.D in Electrical Engineering from Visveswaraya Technological University, Karnataka, India, M.Tech in Control Systems from University of Kerala, in 2001 and Bachelor Degree in Electrical and Electronics Engineering from University of Calicut in 1998. She is currently working as Assistant Professor in the Department of Electrical and Electronics Engineering, Presidency University, Bengaluru, Karnataka. Her research area includes robust control systems, fuzzy logic control, and control of industrial drives. She is a life member of international society for technical education (ISTE) and associate member of institution of engineers. She can be contacted at email: jisha@presidencyuniversity.in.

**Arekkadan Antony Powly Thomas** received her Ph.D in Aerospace Engineering from Indian Institute of Science, Bengaluru in the year 2004, M.Tech in Control Systems from University of Kerala, in 1988 and Bachelor Degree in Electrical Engineering from University of Calicut in 1986. Her research area is robust control system for aerospace applications. She is a Life Member of International Society for Technical Education (ISTE), Fellow of Institution of Engineers (FIE) and IEEE member. She is a member of board of studies (BOS) and board of examinations (BOE) in Visvesvaraya Technological University. She has published several research papers in reputed journals and conferences. She can be contacted at email: drpowlythomas@gmail.com.

**Suresh Srivastava** is a Defence Scientist heading indigenous design, development and certification of airborne surveillance systems in Defence R & D Organisation using end-to-end Aerospace standard AS9100 Quality management system. He has done graduation in Mechanical Engg. from N.I.T, Surat, Fellowship in Gas Turbine Technology from Defence Institute of Advanced Technology, Pune, M.Tech. & Ph.D in Control system design from IIT Bombay. His doctoral research effort was in the field of design of robust control system with application to aero gas turbine engine. He has also served at Indian institute of science for 5 years on deputation. He can be contacted at email: sureshdrdo@yahoo.co.in.